

Aging transition in the absence of inactive oscillators

K. Sathiyadevi,¹ I. Gowthaman,¹ D. V. Senthilkumar,^{2, a)} and V. K. Chandrasekar^{1, b)}

¹⁾Centre for Nonlinear Science & Engineering, School of Electrical & Electronics Engineering, SASTRA Deemed University, Thanjavur - 613 401, Tamil Nadu, India.

²⁾School of Physics, Indian Institute of Science Education and Research, Thiruvananthapuram - 695551, Kerala, India.

(Dated: 2 August 2019)

The role of counter-rotating oscillators in an ensemble of coexisting co- and counter-rotating oscillators is examined by increasing the proportion of the latter. The phenomenon of aging transition was identified at a critical value of the ratio of the counter-rotating oscillators, which was otherwise realized only by increasing the number of inactive oscillators to a large extent. The effect of the mean-field feedback strength in the symmetry preserving coupling is also explored. The parameter space of aging transition was increased abruptly even for a feeble decrease in the feedback strength and subsequently aging transition was observed at a critical value of the feedback strength surprisingly without any counter-rotating oscillators. Further, the study was extended to symmetry breaking coupling using conjugate variables and it was observed that the symmetry breaking coupling can facilitate the onset of aging transition even in the absence of counter-rotating oscillators and for the unit value of the feedback strength. In general, the parameter space of aging transition was found to increase by increasing the frequency of oscillators and by increasing the proportion of the counter-rotating oscillators in both the symmetry preserving and symmetry breaking couplings. Further, the transition from oscillatory to aging transition occurs via a Hopf bifurcation, while the transition from aging transition to oscillation death state emerges via Pitchfork bifurcation. Analytical expressions for the critical ratio of the counter-rotating oscillators are deduced to find the stable boundaries of the aging transition.

Aging is a kind of deterioration which occurs in diverse complex systems. It is evident from our daily life that living organisms (and its efficiency) degrade as it becomes older. For instance, Alzheimer's disease is an example of a cause of failure of neurons due to the aging process. In this context, the phenomenon of aging transition was reported in an ensemble of oscillators by increasing the proportion of inactive oscillator²⁵⁻³⁰. In the present work, we show that even an appropriate proportion of counter-rotating oscillators in an ensemble of coexisting co- and counter-rotating oscillator is capable of inducing the phenomenon of aging transition. Further, we find that either the mean-field feedback or the symmetry breaking coupling alone can facilitate the onset of the aging transition.

in the complex networks, degrading its dynamical activity. In neural networks, de-actuation of a single node may cause series concern in the entire network, which cascades continuous degradation of neighboring nodes^{22,23}. A similar issue has also been reported in the power grids²⁴. Initially, the phenomenon of aging transition was reported by increasing the number of inactive oscillators from the active group of oscillators in a globally coupled network. Originally, the effect of aging behavior was analyzed through globally and diffusively coupled oscillators²⁵⁻²⁸. Further, the emergence of desynchronization horn was identified for sufficiently strong nonisochronicity where the active oscillators desynchronize resulting in local clustering²⁶. The phenomenon of aging transition was also analyzed by different groups probing various aspects of the network^{27,29-31}.

On the other hand, coexisting co- and counter-rotating dynamical activity can be found in various natural systems such as fluid dynamics^{32,33}, physical^{34,35} as well as biological systems³⁶. Hence special attention is deemed towards enriching our knowledge on counter-rotation induced collective dynamics in various systems. Originally, the coexistence of clockwise and anticlockwise rotations was identified by Tabor³⁷. Later, the universal occurrence of mixed synchronization was reported in Stuart-Landau and Rössler oscillators³⁸. Further, mixed synchronization was demonstrated both theoretically as well as experimentally in the various limit cycle and chaotic systems³⁹⁻⁴¹. Very recently, the counter-rotating frequency induced dynamical effects were reported in the coupled Stuart-Landau oscillator with symmetry preserving as well as symmetry breaking couplings. These authors identified the suppression of oscillation death state when the symmetry breaks in the counter-rotating system⁴². In addition, feedback also plays an essential role in the various natural and man-made systems. One of the recent reports demonstrated that by introducing a feedback strength in the

I. INTRODUCTION

Complex systems are abundant, omnipresent in nature and are rarely isolated. Coupled nonlinear oscillators serve as an excellent framework to unravel distinct collective patterns observed in such complex systems, which include chemical^{1,2} and biological systems^{3,4}, and so on. The network architecture and the strength of the interaction of the coupled systems facilitate the onset of various collective behaviors such as synchronization^{5,6}, chimera^{4,7-12}, clustering^{13,14}, and distinct oscillation quenching states¹⁶⁻²¹, having strong resemblance with many natural processes. The phenomenon of aging transition is one such a phenomenon of serious concern

^{a)}Electronic mail: skumarusnd@gmail.com

^{b)}Electronic mail: chandru25nld@gmail.com

coupling can switch the stability of the stable steady states facilitating the revival of oscillation in coupled nonlinear oscillators, which was also further corroborated experimentally using coupled electrochemical oscillators⁴³. The addition of external feedback in retaining and enhancing the dynamical robustness in the presence and absence of time-delay was also reported⁴⁴. In particular, mean-field feedback has a predominant application in neuroscience in deep brain simulation^{45,46}.

Motivated by the above, in this work, we investigate the effect of coexisting co- and counter-rotating oscillators on the emerging collective dynamical behavior of such an ensemble. Further, we also aim to study the impact of the mean-field feedback on the observed collective dynamical behaviors. In order to elucidate the above, we consider an array of globally coupled Stuart-Landau oscillators. Primarily, the effect of the counter-rotating oscillators will be analyzed in symmetry preserving coupling. Surprisingly, we find that the proportion of the counter-rotating oscillators play a vital role in facilitating the onset of aging transition through the Hopf bifurcation, which was otherwise identified only due to increasing in the number of inactive oscillators^{25–30}. The spread of aging transition is found to increase upon increasing the frequency of the oscillators. We have also estimated the critical ratio of the counter-rotating oscillators to show the stable boundaries of the aging transition. In addition, we also investigate the effect of the mean-field feedback on the spread of the aging transition. Interestingly, we find that even a very small decrease in the mean-field feedback strength enhances the aging transition region. In particular, we find that the mean-field induces the phenomenon of aging transition in an ensemble of oscillators even without any counter-rotating oscillators. Further, the robustness of the observed results will be analyzed for symmetry breaking conjugate coupling. We observe that the dynamical transition takes place from oscillatory to oscillation death state via aging transition. We deduce the critical ratio of the counter rotating oscillator to find the stable boundaries of the spread of the aging transition. Enriching the observed results, we find that the conjugate coupling, which breaks the rotational symmetry, indeed induces aging transition via a Hopf bifurcation even without the counter-rotating oscillators and for the unit value of the mean-field feedback. In this case, the mean-field feedback enhances the aging transition region. It is also to be noted that the transition from aging transition to oscillation death takes place through pitchfork bifurcation. We find that the aging transition region enlarges upon decreasing the feedback strength and increasing the frequency of the oscillators.

The rest of the article is organized as follows: We will demonstrate the emergence of the aging transition region through symmetry preserving coupling in Sec. II, where the influence of the mean-field feedback will be discussed. In Sec. III, the robustness of the obtained results will be inspected in a symmetry breaking conjugate coupling as well. Finally, we summarize our results and draw conclusions in Sec. IV.

II. AGING TRANSITION: SYMMETRY PRESERVING COUPLING

To find the impact of the counter-rotating oscillators in inducing the aging transition, we consider a general paradigmatic model of Stuart-Landau limit cycle oscillators with symmetry preserving coupling. Various natural phenomena including the breathing cycle, the circadian clock shows the limit cycle behavior. Many nonlinear dynamical systems near the Hopf bifurcation can be approximated through Stuart-Landau oscillator^{47–49}. An array of globally coupled Stuart-Landau oscillators with symmetry preserving coupling can be written as

$$\dot{z}_j = (\lambda + i\omega_j - |z_j|^2)z_j + \frac{K}{N} \sum_{k=1}^N (\alpha z_k - z_j), \quad (1)$$

where $z_j = re^{i\theta_j} = x_j + iy_j \in \mathbb{C}$, $j = 1, 2, \dots, N$. N be the number of elements in the network which is chosen as $N = 100$. x_j and y_j are the state variables of the j^{th} system. λ is the Hopf bifurcation parameter and α is the mean-field feedback strength. ω_j is the frequency of the j^{th} system. If the system frequency is $+\omega$, the system rotates in a counter-clockwise direction, while $-\omega$ indicates the clockwise direction. In order to study the role of the counter-rotating oscillators, we split the oscillators as one group of oscillators with the system frequency $\omega_j = \omega$ for $j \in 1, \dots, N(1-p)$ while the other group takes the value, $\omega_j = -\omega$ for $j \in N(1-p) + 1, \dots, N$. The parameter p characterizes the fraction of the counter rotating oscillators. Now, we investigate the emergence of the aging transition as a function of the ratio of the counter rotating oscillators. The numerical analysis of the system (1) is carried out using Runge-Kutta fourth order scheme with step size 0.01 time units.

Initially, to unravel the onset of the aging transition as a function of the ratio of the counter-rotating oscillators, we estimate the order parameter $|Z|$, where $Z = \frac{1}{N} \sum_{j=1}^N z_j$, as in refs.^{25–30}. Then the normalized order parameter can be expressed as, $Q \equiv |Z(p)|/|Z(0)|$. p is the ratio of the counter-rotating oscillators. $p = 0$ and $p = 1$, respectively, denotes the completely counter-clockwise and clockwise rotating oscillators while $p = 0.5$ indicates the equal ratio of co- and counter-rotating oscillators. The coupled Stuart-Landau oscillator (1), manifests symmetric dynamical transitions either by increasing the ratio of the counter-rotating oscillators from the range $p \in (0, 0.5)$ to $p \in (0.5, 1)$ or decreasing it from $p \in (1, 0.5)$ to $p \in (0.5, 0)$. Hence, we examine the effect of the counter-rotating oscillator ratio from $p = 0$ to $p = 0.5$ throughout our study.

To delineate the emergence of the aging transition, we have plotted the normalized order parameter (Q) as a function the ratio of the counter-rotating oscillators (p) for two different values of the mean-field feedback strength (α) in Figs. 1(a) and 1(b). In order to exemplify the above, we fix the system frequency $\omega = 5.0$. Finite non-zero value of the normalized order parameter is observed in the entire range of p for $K = 1.0$, elucidating the oscillatory nature of the dynamical state of all the oscillators. It is observed that the

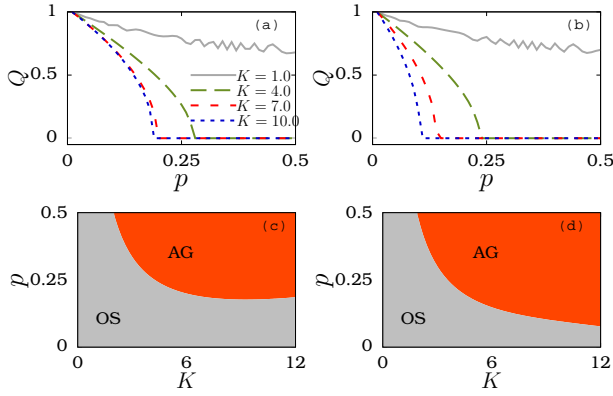


FIG. 1. Normalized order parameter (Q) as a function of the ratio of the counter-rotating oscillators (p) for (a) $\alpha = 1.0$ and (b) $\alpha = 0.95$, by fixing $\omega = 5.0$, $\lambda = 1.0$ and $N = 100$. The distinct line types denotes the coupling strengths $K = 1.0$, 4.0 , 7.0 and $K = 10.0$. The corresponding two parameter diagram in (K, p) space as a function of the coupling strength are depicted in Figs. (c) and (d). OS and AG represent the oscillatory and the aging transition region.

normalized order parameter transit from finite value to null value at the critical values $p_{HB} = 0.28$, 0.2 , and 0.19 , for the coupling strengths $K = 4.0$, 7.0 , and 10.0 , respectively. The null value of Q indicates the existence of the aging transition region, which emerges through the Hopf bifurcation. From Fig. 1(a), it is also evident that increasing the coupling strength decreases the critical value p_{HB} , thereby illustrating that the aging transition emerges even for smaller proportion of the counter-rotating oscillators, enhancing the aging transition region, in strong contrast to increasing the number of inactive oscillators to realize the aging transition as reported so far^{25,26}. Further, to unravel the influence of the mean-field feedback on the aging transition, we have also depicted the normalized order parameter for $\alpha = 0.95$ in Fig. 1(b). The coupled systems exhibit oscillatory behavior for $K = 1$. When increasing the coupling strength to $K = 4.0$, 7.0 , and 10.0 , the onset of the aging transition take place at $p_c = 0.24$, 0.15 and 0.1 , respectively. Thus, it is evident from both Figs. 1(a) and 1(b) that the critical value of p_{HB} , for the onset the aging transition, abruptly decreases even for a feeble decrease in the mean-field feedback strength α , enhancing the aging transition region. The corresponding global behavior of the coupled co- and counter-rotating system (1) is depicted in Figs. 1(c) and 1(d) in (K, p) space for $\alpha = 1.0$ and $\alpha = 0.95$, respectively. The co- and counter-rotating coupled Stuart-Landau oscillators exhibit oscillations for small values of the coupling strength and for the smaller ratio of the counter-rotating oscillators, whereas the coupled Stuart-Landau oscillators shows the aging transition for appreciable values of p and K (see Figs. 1(c) and 1(d)). Further, to confirm the emergence of aging transition analytically, we have performed the linear stability analysis which will be detailed as follows.

In the aging transition, z_j is stabilized to trivial fixed point (i.e. $z_j = 0$). We assume that the coupled system (1) subdivided into two groups, similar to the case of active-inactive

group of oscillators as in ref.²⁵. Here, one group $w_1 = z_j$, ($j = 1, \dots, N(1-p)$) rotates in clockwise direction while the other group $w_2 = z_j$, ($j = N(1-p) + 1, \dots, N$) rotates in counter-clockwise direction.

$$\begin{aligned} \dot{w}_1 &= (1 + i\omega - |w_1|^2)w_1 + K(\alpha(1-p)w_2 - (1-\alpha p)w_1), \\ \dot{w}_2 &= (1 - i\omega - |w_2|^2)w_2 + K(\alpha p w_1 + (\alpha(1-p) - 1)w_2) \end{aligned} \quad (2)$$

It is to be noted that the sign of ω , either positive or negative depicts whether the oscillators are rotating in clockwise or anti-clockwise direction, respectively. By performing the linear stability analysis of Eq. (2) around the origin ($w_1 = w_2 = 0$), one can obtain an expression for the critical ratio of the counter rotating oscillators p_{HB} as

$$p_{HB} = \frac{\alpha^2 K^2 (2 + (-2 + \alpha)K)^2 \omega^2 \pm \sqrt{\Delta_1}}{(2\alpha^2 K^2 (2 + (-2 + \alpha)K)^2 \omega^2)}. \quad (3)$$

where, $\Delta_1 = \alpha^2 K^2 (2 + (-2 + \alpha)K)^6 \omega^2 (-1 - (-2 + \alpha)k + (-1 + \alpha)K^2 - \omega^2)$. Using the above expression, one can ob-

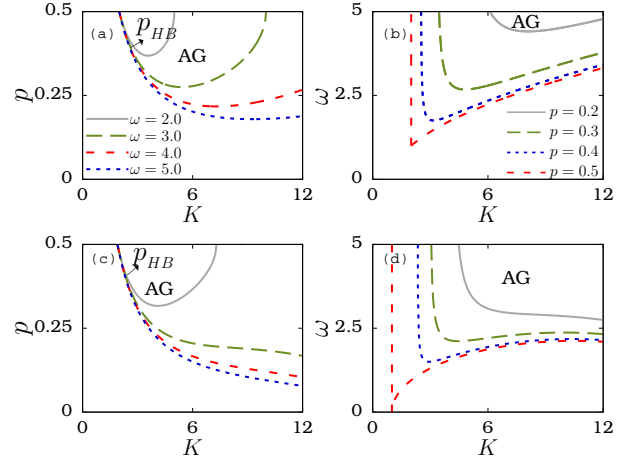


FIG. 2. Analytical boundaries of the aging transition region for $\alpha = 1.0$: (a) (K, p) space for different values of system frequency $\omega = 2.0$, 3.0 , 4.0 and 5.0 . (b) (K, ω) space for different values of the critical ratio of the counter rotating oscillators p for $p = 0.2, 0.3, 0.4$ and $p = 0.5$. p_{HB} is the critical curve corresponding to Hopf bifurcation curve. The corresponding analytical aging boundaries for $\alpha = 0.95$ are shown in Fig. (c) and (d).

tain the stable boundaries of the aging transition region as depicted in Fig. 2. The critical curve p_{HB} is the Hopf bifurcation curve across which there is a change the stability of the limit cycle occurs. Figures 2(a) and 2(b) are plotted for the mean-field feedback $\alpha = 1.0$. The distinct line-types in Fig. 2(a) correspond to the different values of ω , namely as $\omega = 2.0$, $\omega = 3.0$, $\omega = 4.0$ and $\omega = 5.0$ in (K, p) plane. From Fig. 2(a), it is evident that increasing the system frequency increases the aging transition region as a function of the coupling strength and the ratio of the counter-rotating oscillators. Similarly, the aging transition regions are depicted in (K, ω) plane in Figure 2(b) for different ratio of the counter rotating oscillators $p = 0.2$, $p = 0.3$, $p = 0.4$ and $p = 0.5$. The

region enclosed by the curves correspond to aging transition region. Figure 2(b) clearly delineates the increase in the aging transition region while increasing the ratio of counter-rotating oscillators. Moreover, the aging transition region enhances to a large extent when both the co- and counter-rotating oscillators balance each other. Further, to substantiate the observed results in Fig. 1, we have also depicted the dynamical transition observed for the mean-field feedback $\alpha = 0.95$. Thus, it is evident from Figs. 2(c) and 2(d) that the aging transition region is increased upon decreasing the mean-field feedback strength α . In particular, the aging transition region enhances for increasing the frequency of the oscillations, increasing the ratio of the counter-rotating oscillators and while decreasing the mean-field feedback strength.

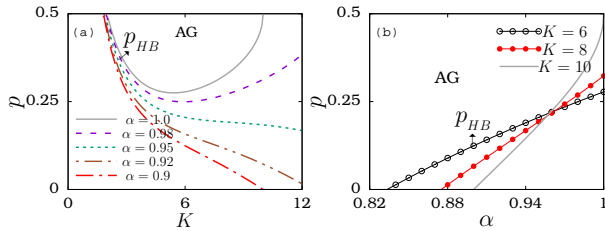


FIG. 3. (a) The aging transition region, for symmetry preserving coupling, for different values of the mean-field feedback strength ($\alpha = 1.0, 0.98, 0.95, 0.92$ and 0.9) for the system frequency $\omega = 3.0$. (b) Critical ratio of counter rotating oscillators as a function of the feedback strength for the system frequency $\omega = 3.0$ and the coupling strengths $K = 6.0, K = 8.0$ and $K = 10.0$.

For further insight on the effect of the mean-field feedback strength on the aging transition region and to show the enlarging of the aging transition region as a function of the feedback strength, we have depicted the critical boundaries p_{HB} of the aging transition for $\omega = 3.0$ in Fig. 3(a). The boundaries are plotted for the values of the feedback strength $\alpha = 1.0, 0.97, 0.95, 0.92$ and 0.9 which clearly depicts the increase in the aging transition region for decreasing values of the feedback strength. Further, the observed results are validated by finding the critical value p_c as a function of α for three different values of the coupling strengths $K = 6.0, K = 8.0$ and $K = 10.0$ as shown in Fig. 3(b). Lines connected by open circles, filled circles and solid line correspond to the coupling strength $K = 6.0, K = 8.0$ and $K = 10.0$, respectively. It is evident that the critical value p_c facilitating the onset of the aging transition region drops down to zero even for a small decrease in the mean-field feedback strengths. Substantiating that the aging transition can indeed be induced by the mean-field feedback strength even in the absence of the counter-rotating oscillators. One can also note that increasing the coupling strength decreases the value of the mean-field feedback strength for the onset of the aging transition.

From symmetry preserving coupling, we have unraveled the emergence of the aging transition via Hopf bifurcation as a result of increasing the ratio of the counter-rotating oscillators. It is also established that the mean-field feedback can facilitate the onset of the aging transition without any counter-rotating oscillators. In addition, the spread of the aging transition re-

gion is increased upon either increasing the system frequency or decreasing the mean-field feedback strength. Further, to examine the robustness of the observed transition, we have also analyzed the dynamical transitions in a symmetry breaking coupling in the following.

III. AGING TRANSITION: SYMMETRY BREAKING COUPLING

It is an established fact that the symmetry breaking coupling can be responsible for the emergence of various collective patterns including frequency cluster, amplitude cluster, amplitude chimera, frequency chimera, various kinds of oscillation quenching states and so on^{8,50,51}. We introduce the symmetry breaking in the coupling using the conjugate variables in the coupling. In this section, we investigate the effect of conjugate coupling on the aging transition as a function of the counter-rotating oscillators, the frequency of the oscillators, and the mean-field feedback. In order to illustrate the above, we consider an array of globally coupled Stuart-Landau oscillators with conjugate coupling described as

$$\dot{z}_j = (\lambda + i\omega_j - |z_j|^2)z_j + \frac{K}{N} \sum_{k=1}^N (\alpha \text{Im}(z_k) - \text{Re}(z_j)). \quad (4)$$

Here, the coupling among the oscillators is implemented through dissimilar variables. The proposed coupling breaks the system rotational symmetry explicitly, where the rotational invariance is not preserved under such transformation $z_j \rightarrow z_j e^{i\theta}$.

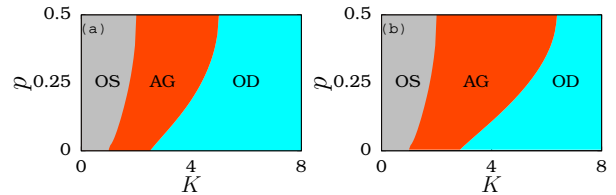


FIG. 4. Two parameter diagram for an array of conjugately coupled Stuart-Landau oscillators (symmetry breaking coupling) in (K, p) space for (a) $\alpha = 1.0$ and (b) $\alpha = 0.96$. Other parameters: $\lambda = 1.0, \omega = 2.0$ and $N = 100$. OS, AG and OD represent the oscillatory, aging transition state and oscillation death state, respectively.

Initially, the dynamical transitions are analyzed numerically as a function of the coupling strength in symmetry breaking conjugately coupled system (4). Figures 4(a) and 4(b) are plotted for two different values of the mean-field feedback strength $\alpha = 1.0$ and $\alpha = 0.96$, respectively, for the system frequency $\omega = 2.0$. From both the figures, we found that the transition takes place from oscillatory region to oscillation death state through the aging transition. The transition from oscillatory to aging transition transition takes place via Hopf bifurcation while transit from aging to oscillation death occurs via pitchfork bifurcation. Further, it is to be noted that the symmetry breaking coupling using the conjugate variables

induces the aging transition without any counter-rotating oscillators even for the unit value of the mean-field feedback strength. Comparing Fig. 4(b) with Fig. 4(a), it is clear that the feedback strength α increases the aging transition region in the (K, p) space but the oscillatory region remains unaltered. Furthermore, the observed numerical boundaries of the aging transition region are confirmed analytically in the following.

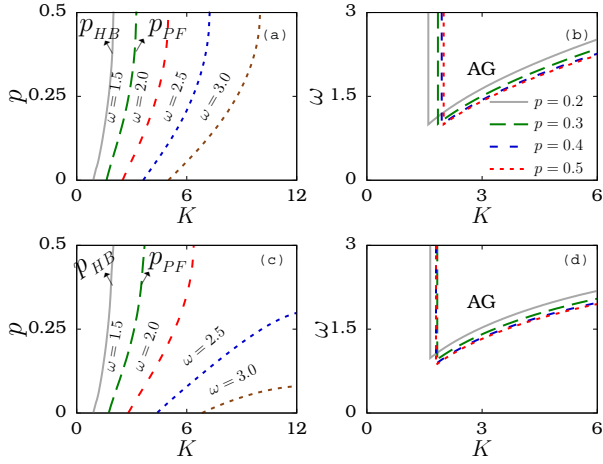


FIG. 5. Analytical boundaries of the aging transition region (a) (K, p) plane for distinct values of the system frequency $\omega = 2.0, 3.0, 4.0$ and 5.0 and (b) (K, ω) plane for $p = 0.2, 0.3, 0.4$ and $p = 0.5$. p_{HB} and p_{PF} are the critical value of the counter rotating oscillators, which separate the boundary between the oscillatory and the aging transition region, and the aging transition and the oscillation death, respectively. The corresponding analytical boundaries for $\alpha = 0.96$ is shown in Fig. (c) and (d).

For finding the analytical boundaries of the aging transition region in the symmetry breaking conjugate coupling, we have deduced the critical ratio of the counter rotating oscillators from the linear stability analysis as,

$$p_{HB} = \frac{(2\alpha^2(-1+K)^2K^2w^2 \pm \sqrt{\Delta_2})}{4\alpha^2(-1+K)^2K^2w^2}, \quad (5)$$

and

$$p_{PF} = \frac{\alpha^2K^2\omega^2 \pm \sqrt{\Delta_3}}{2\alpha^2K^2w^2}, \quad (6)$$

where $\Delta_2 = \alpha^2(-1+k)^4K^2(4-8K-(-4+\alpha^2)K^2)\omega^2(8K+(-4+\alpha^2)K^2-4(1+\omega^2))$, and $\Delta_3 = \alpha^2K^2\omega^2((\alpha^2-1)K^4-2(\alpha^2-2)K^3+(\alpha^2-6-2\omega^2)+4K(1+\omega^2)-(1+\omega^2)^2)$. p_{HB} and p_{PF} are the critical curves corresponding to the Hopf bifurcation and the pitchfork bifurcation curves. Across p_{HB} there is a change in the stability of the limit cycle oscillators, which separate the boundary between the oscillatory state and the aging transition region. p_{PF} is the pitchfork bifurcation curve on which there is a transition from homogeneous steady state (AT) to inhomogeneous steady state (OD state). Using Eq. (5) and Eq. (6), we have plotted Fig. 5 in (K, p) space and (K, ω) space. Enhancing of the aging transition region

is clearly evident (see Fig. 5(c) and 5(d)) for decrease in the value of the mean-field strength.

Finally, to show the nature of the aging transition region upon decreasing the mean-field feedback strength in the symmetry breaking coupling, we have depicted the analytical curves of different mean-field feedback strength $\alpha = 1.0, 0.98, 0.96, 0.94$ for $\omega = 2.0$ and $\omega = 2.5$ in Figs. 6. It is evident from Figs. 6(a) and 6(b) that the aging transition region increases upon increasing the frequency of the oscillators and decreasing the mean-field feedback strength. Further, it is also evident that decreasing the feedback strength to ($\alpha = 1.0, 0.98, 0.96, 0.94$) increases the aging transition region.

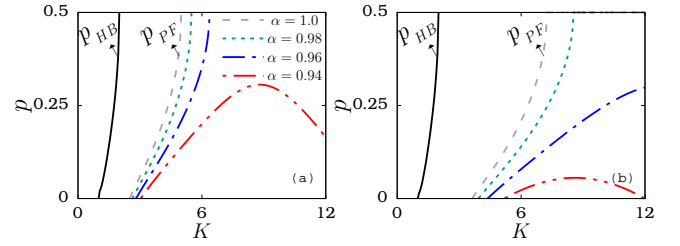


FIG. 6. The aging transition region for the different value of the feedback strength in conjugately coupled Stuart-Landau oscillators. Analytical boundaries of the aging transition region for distinct values of feedback strength ($\alpha = 1.0, 0.98, 0.96, 0.94$) for (a) $\omega = 2.0$ and (b) $\omega = 2.5$.

From the above discussed results from the symmetry preserving and symmetry breaking coupling, it is confirmed that even the proportion of the counter-rotating oscillator in an ensemble of coexisting co- and counter-rotating oscillators, indeed, facilitates the emergence of the aging transition in contrast to the earlier reports, where a large proportion of inactive oscillators are introduced to realize the same. In addition, it is shown that the mean-field feedback strength facilitates the onset of the aging transition despite the absence of the counter-rotating oscillators. Region of the observed aging transition is enhanced while increasing the frequency of the system or decreasing the mean-field feedback strength. Further, it is clear that such transition is robust in both symmetry preserving as well symmetry breaking coupled oscillators.

IV. CONCLUSION

Degradation of dynamical activity (is also called as aging) is inevitable in many complex networks including power grids and neural networks. In the present work, we have explored the onset of the aging transition in a network of the globally coupled limit cycle oscillators where the system frequencies are distributed to a distinct ratio of co- and counter-rotating oscillators. We found that even the counter-rotating oscillators also can induce the aging transition in an ensemble of coexisting co- and counter-rotating oscillators unlike the earlier reports, which increases a large proportion of the inactive oscillators. In order to show this, initially, we have considered

an array of globally coupled Stuart-Landau limit cycle oscillators with symmetry preserving coupling. We have analyzed the influence of the mean-field feedback strength on the aging transition. Interestingly, we have observed that aging transition region is enhanced abruptly even for a small decrease in the feedback strength and subsequently the ratio of the counter-rotating oscillators necessary to induce the aging transition drops down to zero corroborating that the mean-field feedback can indeed induce the phenomenon of the aging transition. Further, we have also analyzed the effect of the system frequency on the aging transition region, which increases the aging transition region. The observed results are further confirmed analytically through the linear stability analysis by deducing the critical ratio of the counter-rotating oscillators for which change in the stability of the limit cycle oscillators occurs via the Hopf bifurcation. Additionally, the robustness of such aging transition is also analyzed in the symmetry breaking conjugate coupling which also exhibits similar dynamical transitions. Surprisingly, we found that the symmetry breaking conjugate coupling itself is capable of facilitating the onset of the aging transition without any counter-rotating oscillators even for the unit value of the mean-field feedback strength. Furthermore, we have also deduced the analytical critical curves corresponding to the Hopf bifurcation and the pitchfork bifurcation curves. Finally, from the obtained results, we have identified that the observed aging transition behavior is robust in both symmetry preserving as well as symmetry breaking coupling.

The proposed work also leads to many open problems. Due to complex interactions in real-world systems, the study of collective dynamics under distinct network geometries is intriguing research for many years and is inevitable. Therefore, it is a valuable insight to extend our analysis to various topological structures including scale-free, small world and so on^{26,30}. Since, feedback is a general mechanism to revoke the dynamism from the deteriorated dynamical units in a complex network and is also essential to investigate the influence of various feedbacks^{43,52-54}. From the earlier reports, it is identified that the processing delay is used to destabilize the homogeneous as well as an inhomogeneous steady state either in the presence or the absence of propagation delay^{55,56}. Thus, it will also be interesting to investigate the effect of various delays including propagation delay, processing delay, and low pass filter^{43,52,54-57}. Furthermore, the role of nonlinear parameter is invident in the observed dynamical transitions and which plays a crucial role in inducing various collective patterns^{8,26,27,51}. In view of the above, it is also intriguing to investigate the dynamical transition with the addition of nonisochronicity parameter, as a function of co- and counter-rotating frequencies of a dynamical system.

ACKNOWLEDGMENTS

KS sincerely thanks the CSIR for a fellowship under SRF Scheme (09/1095(0037)/18-EMR-I). The work of VKC supported by a research project CSIR under Grant

No.03(14444)/18/EMR-II. DVS is supported by the CSIR EMR Grant No. 03(1400)/17/EMR-II. We also thank the SASTRA Deemed university for providing good infrastructure lab facilities.

- ¹Y. Kuramoto, *Chemical Oscillations, Waves, and Turbulence*, Springer-Verlag Berlin Heidelberg (1984).
- ²R. Toth, A. F. Taylor, and M. R. Tinsley, *J. Phys. Chem. B*, **110**, 10170-10176, (2006).
- ³J. Sawicki, I. Omelchenko, A. Zakharova and E. Schöll, *Euro. Phys. J. B* **92**, 54 (2019).
- ⁴S. Majhi, B. K. Bera, D. Ghosh, and M. Perc, *Phys. Life Rev.* **28**, 100-121 (2019).
- ⁵A. Pikovsky, M. G. Rosenblum, and J. Kurths, *Synchronization: A Universal Concept in Nonlinear Sciences* (Cambridge University Press, Cambridge, 2001).
- ⁶S. Gupta, A. Campa, and S. Ruffo, *Statistical Physics of Synchronization*, Springer Briefs in Complexity, Springer International Publishing, (2018).
- ⁷M. Panaggio and D. M. Abrams, *Nonlinearity* **28**, R67-R87 (2015).
- ⁸A. Zakharova, M. Kapeller, and E. Schöll, *Phys. Rev. Lett.* **112**, 154101 (2014).
- ⁹I. Omelchenko, A. Provata, J. Hizanidis, E. Schöll, and P. Hövel, *Phys. Rev. E* **91**, 022917 (2015).
- ¹⁰E. Schöll, *Eur. Phys. J. Special Topics* **225**, 891-919 (2016).
- ¹¹K. Sathiyadevi, V. K. Chandrasekar, and D. V. Senthilkumar, *Phys. Rev. E* **98**, 032301 (2018).
- ¹²S. Ghosha, A. Zakharova, and S. Jalan, *Chaos, Solitons & Fractals* **106**, 56-60 (2018).
- ¹³S. Gil, Y. Kuramoto, and A. S. Mikhailov *Europhys. Lett.* **88**, 60005 (2009).
- ¹⁴K. Sathiyadevi, V. K. Chandrasekar, D. V. Senthilkumar, and M. Lakshmanan, *Phys. Rev. E* **97**, 032207 (2018).
- ¹⁵G. Saxena, A. Prasada, and R. Ramaswamy, *Phys. Rep.* **521**, 205-228 (2012).
- ¹⁶A. Koseska, E. Volkov, and J. Kurths, *Phys. Rep.* **531**, 173-199 (2013).
- ¹⁷T. Banerjee and D. Ghosh, *Phys. Rev. E* **89** (5), 052912 (2014).
- ¹⁸I. Schneider, M. Kapeller, S. Loos, A. Zakharova, B. Fiedler, and E. Schöll, *Phys. Rev. E* **92**, 052915 (2015).
- ¹⁹W. Zou, M. Zhan, and J. Kurths, *Phys. Rev. E* **98**, 062209 (2018).
- ²⁰V. Resmi, G. Ambika, and R. E. Amritkar, *Phys. Rev. E* **84**, 046212 (2011).
- ²¹A. Sharma, P. R. Sharma and M. D. Shrimali, *Phys. Lett. A* **376**, 1562-1566 (2012).
- ²²L. Ambrogioni, M. A. J. vanGerven, E. Maris, *PLoS Comput. Biol.* **13**(5), e1005540 (2017).
- ²³S. Atasoy, L. Roseman, M. Kaelen, M. L. Kringelbach, G. Deco, R. L. Carhart-Harris, *Sci. Rep.* **7**, 17661 (2017).
- ²⁴C. L. DeMarco, *IEEE Control Syst. Mag.* **21**, 40-51 (2001).
- ²⁵H. Daido and K. Nakanishi, *Phys. Rev. Lett.* **93**, 10 (2004).
- ²⁶H. Daido and K. Nakanishi, *Phys. Rev. E* **75**, 056206 (2007).
- ²⁷H. Daido, *Europhysics. Lett.* **87**, 40001 (2009).
- ²⁸G. Tanaka, K. Morino, H. Daido, and K. Aihara, *Phys. Rev. E* **89**, 052906 (2014).
- ²⁹B. Thakur, D. Sharma, and A. Sen, *Phys. Rev. E* **90**, 042904 (2014).
- ³⁰S. Kundu, S. Majhi, P. Karmakar, D. Ghosh and B. Rakshit, *Euro. Phys. Lett.* **123**, 30001 (2018).
- ³¹R. Mukherjee and A. Sen, *Chaos* **28**, 053109 (2018);
- ³²Y. Murakami and H. Fukuta, *Fluid Dyn. Res.* **21** 1-12 (2002); H. Fukuta, Y. Murakami, *Phys. Rev. E* **57**, 449-59 (1998).
- ³³M. Darvishyadegari and R. Hassanzadeh, *Acta Mech.* **229**, 1783-1802 (2018).
- ³⁴K. Czolczynski, P. Perlikowski, A. Stefanski and T. Kapitaniak, *Commun. Nonlinear Sci. Numer. Simulat.* **17**, 3658-72 (2012).
- ³⁵J. Strzalko, J. Grabski, J. Wojewoda, M. Wiercigroch, and T. Kapitaniak, *Chaos* **22**, 047503 (2012).
- ³⁶S. Takagi and T. Ueda *Physica D* **237**, 420-7 (2008).
- ³⁷M. Tabor, *Chaos and Integrability in Nonlinear Dynamics: An Introduction*. John Wiley & Sons, New York; 1988.
- ³⁸A. Prasad, *Chaos, Solitons and Fractals* **43**, 42-46 (2010).
- ³⁹S. K. Bhowmick, D. Ghosh, and S. K. Dana, *Chaos* **21** 033118 (2011).
- ⁴⁰A. Sharma and M. D. Shrimali, *Nonlinear Dyn.* **69**, 371-377 (2012).

- ⁴¹B. K. Bera, S. K. Bhowmick and D. Ghose, *Int. J. Dynam. Control*, **5**, 269–273 (2017).
- ⁴²N. Punetha, V. Varshney, S. Sahoo, G. Saxena, A. Prasad and R. Ramaswamy, *Phys. Rev. E* **98**, 022212 (2018).
- ⁴³W. Zou, D. V. Senthikumar, R. Nagao, I. Z. Kiss, Y. Tang, A. Koseska, J. Duan and J. Kurths, *Nat. Commun.* **6**, 7709 (2015).
- ⁴⁴S. Kundu, S. Majhi, and D. Ghosh, *Phys. Rev. E* **97**, 052313 (2018).
- ⁴⁵A. Franci, A. Chaillet, E. Panteley and F. L. Lagarrigue, *Math. Control Signals Syst.* **24**, 169–217 (2012).
- ⁴⁶M. Luo, Y. Wu and J. Peng, *Biol. Cybern.* **101**, 241–246 (2009).
- ⁴⁷M. Frasca, A. Bergner, J. Kurths and L. Fortuna, *Int. J. Bifurcat. Chaos*, **22**, 1250173 (2012).
- ⁴⁸M. C. Thompson and P. L. Gal, *Eur. J. Mech. B* **23**, 219 (2004).
- ⁴⁹I. Schneider, M. Kapeller, S. Loos, A. Zakharova, B. Fiedler, and E. Schöll, *Phys. Rev. E* **92**, 052915 (2015).
- ⁵⁰Nannan Zhao, Zhongkui Sun and Wei Xu, *Sci. Rep.* **8**, 8721 (2018).
- ⁵¹K. Premalatha, V. K. Chandrasekar, M. Senthilvelan and M. Lakshmanan, *Phys. Rev. E* **91**, 052915 (2015).
- ⁵²V. K. Chandrasekar, S. Karthiga, and M. Lakshmanan, *Phys. Rev. E* **92**, 012903 (2015).
- ⁵³Y. Liu, W. Zou, M. Zhan, J. Duan and J. Kurths, *Europhysics. Lett.* **114**, 40004 (2016).
- ⁵⁴K. Ponrasu, K. Sathiyadevi, V. K. Chandrasekar and M. Lakshmanan *Europhys. Lett.* **124**, 20007 (2018).
- ⁵⁵W. Zou, M. Zhan, and J. Kurths, *Chaos* **27**, 114303 (2017).
- ⁵⁶W. Zou, J. L. O. Espindola, D. V. Senthikumar, I. Z. Kiss, M. Zhan and J. Kurths, *Phys. Rev. E* **99**, 032214 (2019).
- ⁵⁷X. Lei, W. Liu, W. Zou, and J. Kurths, *Chaos* **29**, 073110 (2019)